

1. INTRODUCTION

On GMT 2025-08-02, the SpaceX Dragon Crew-11 vehicle docked to the zenith "top" port of Node2 of the International Space Station (ISS). After docking, the whole orbital platform got a bit bigger and it got a whole lot heavier. Together with its new visiting vehicle, the ensemble now tips the scales at well over a million pounds. The numbers shake out approximately like so:

$$\begin{aligned} \text{Dragon} + \text{ISS}_{\text{before}} &= \text{ISS}_{\text{after}}, \\ 12\,500\text{kg} + 484\,200\text{kg} &= 496\,700\text{kg}. \end{aligned}$$

During vehicle docking or berthing, the ISS holds its usual flight attitude as depicted in Figure 2, an established Torque Equilibrium Attitude (TEA). This specific orientation minimizes external forces like atmospheric drag or gravity gradient, allowing the Control Moment Gyroscopes (CMGs) to keep the station steady without using thrusters. This thruster-free hold lasts for at least a few minutes during the critical final approach, preventing plume impingement and disturbances to the incoming vehicle or the station's solar arrays. This attitude is held constant relative to the rotating Local Vertical Local Horizontal (LVLH) frame – not an inertial frame for any Einsteins reading this. For the final docking stages, the entire attitude control system is often inhibited, putting the station into a "free drift" mode to prevent any unintended thruster firings. All these procedures are governed by flight rules to ensure safety.

This document shows analysis of multiple sensor heads from the Space Acceleration Measurement System (SAMS), which focuses on the vibratory regime of the microgravity environment. It also shows the impact of the Dragon docking as measured by the Microgravity Acceleration Measurement System (MAMS), which measures the ultra-low frequency and magnitude, or so-called quasi-steady regime of the ISS environment.

2. QUALIFY

In this document, we will briefly characterize some key vibratory signal features associated with the Crew-11 Dragon docking event on GMT 2025-08-02. At the time, we note that eight SAMS sensor heads distributed throughout the space station were collecting data at the time of the docking. While these sensor heads have a passband of at least 200 Hz (some at 204.2 Hz) for their triaxial (XYZ) acceleration measurements, we take a first look via a color spectrogram below 6 Hz from

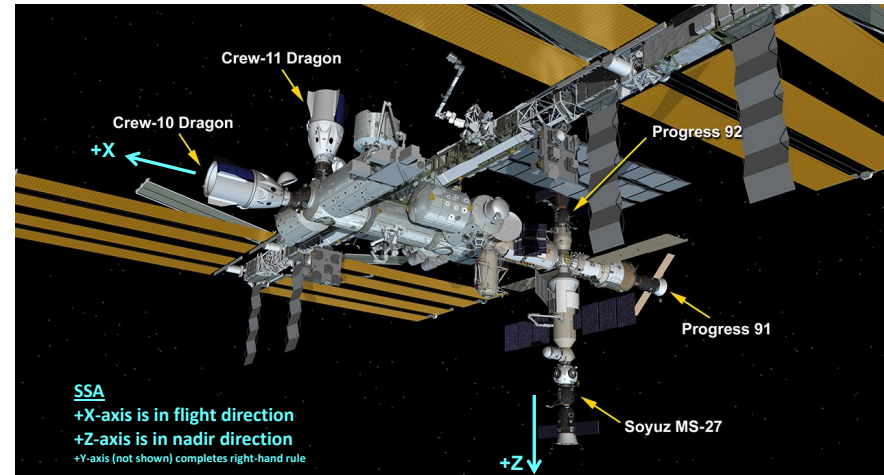


Fig. 1: The ISS After The Crew-11 Dragon Docking on GMT 2025-08-02.

measurements made by the SAMS 121f02 sensor head mounted on the Columbus endcone.

Spectrogram with Vibratory Context for Dragon Docking Event

Figure 3 on page 4 shows a color spectrogram computed from the SAMS sensor head (S/N 121f02) data recorded on the Columbus Starboard Endcone. This spectrogram is intended to show frequency domain features primarily for the structural mode regime over a 12-hour span starting during crew sleep. There are 4 downward pointing arrows annotating signal features in that spectrogram as follows:

- 1) black arrow when Urine Processing Assembly's 3.6 Hz signature turns off
- 2) 2 blue arrows that bound the Russian Segment attitude control span
- 3) magenta arrow when the docking event occurred at about GMT 06:27

Note especially from this spectrogram that the structural mode vibrations (horizontal streaks) between about 1 and 2 Hz flare up as the large structures of the space station with natural frequencies in this range ring out from the impulse of a heavy Dragon impacting the ISS from above.

3. QUANTIFY

In this section, we aim to quantify the impact of the Crew-11 Dragon docking event by first focusing on just a key portion of the acceleration spectrum. We routinely filter SAMS data below 6 Hz for use by structural analysts in the Loads & Dynamics group in Houston and so we tap into those results to highlight a salient feature of such a docking in the vibratory regime.

Per-Axis & Vector Magnitude Acceleration vs. Time Below 6 Hz

The 8 figures for each of 8 SAMS sensor heads distributed throughout the space station and operating at the time of the docking event are enumerated below in Table 1 where we note the cutoff (low-pass) frequency and the xyz per-axis y-limits for the plot so this table can be compared to a similar one later in Table 2. Note in this first table the red horizontal line, which separates the sensors located outside the US Lab. Above the line are sensors in the Columbus and Kibo modules, where the docking event is slightly more impactful and a bit more discernible.

Table 1. SAMS Locations and Figures for 6 Hz Low-Pass Filtered Data.

Fig.	Sensor	Location	Cutoff (Hz)	Y-Limits
4	121f02	COL Endcone	6	±2
5	121f08	COL1A3 (EPM)	6	±2
6	121f05	JPM1F1 (ER5)	6	±2
7	es19	JPM1F6 (ER4)	6	±2
8	121f03	LAB1O1 (ER2)	6	±2
9	121f04	LAB1P2 (ER7)	6	±2
10	es18	LAB1O3 (ER6)	6	±2
11	es20	LAB1S2 (MSG)	6	±2

You will notice in each figure a vertical, dashed, magenta line marking the time of the docking impulse. If you flip back-and-forth among these plots you will notice:

- initial impulsive acceleration direction aligned with +Z-axis
- magenta dashed line when the docking event occurred at about GMT 06:27

- all SAMS sensors are in agreement on when docking occurred¹

Per-Axis & Vector Magnitude Acceleration vs. Time Below 200 Hz

For a one-to-one correspondence with Table 1, we also show Table 2 for the 200 Hz (as-measured) data sets too where you will note the docking event becomes much less discernible or not at all for some sensors:

Table 2. SAMS Locations and Figures for 200 Hz As-Measured Data.

Fig.	Sensor	Location	Cutoff (Hz)	Y-Limits
12	121f02	COL Endcone	200	±10
13	121f08	COL1A3 (EPM)	200	±10
14	121f05	JPM1F1 (ER5)	200	±10
15	es19	JPM1F6 (ER4)	200	±50
16	121f03	LAB1O1 (ER2)	200	±10
17	121f04	LAB1P2 (ER7)	200	±10
18	es18	LAB1O3 (ER6)	200	±40
19	es20	LAB1S2 (MSG)	200	±10

Each figure again includes a vertical dashed magenta line indicating the time of the docking impulse for reference. In the higher-frequency (nominally 200 Hz) passband of the SAMS sensors, localized equipment disturbances often dominate and obscure the docking event signature, as shown in these plots to varying degrees. Two of the more notable disturbance sources during this span were:

- ICEBERG-1 in JPM1F6 (ER-4), which increased the y-limits for es19 to ±50
- GLACIER-2 in LAB1O3 (ER-6), which increased the y-limits for es18 to ±40

A final note from these 200 Hz figures, the 2 SAMS sensor heads in the Columbus module and the es20 sensor head on the Microgravity Science Glovebox (MSG) seat track all showed some signs of the docking event in the Z-axis component of their data.

¹Thanks to Network Time Protocol (NTP), the independent SAMS sensor heads are actively synchronized to a common time source.

Per-Axis Quasi-Steady Impact as Measured by MAMS

The left side image in Figure 20 on page 21 shows what is our routine processing for acceleration archival as "best trimmed-mean-filtered" data. This routine processing is a robust statistical method designed to mitigate the influence of outliers. This process operates on 16-second intervals of raw measurements, and we discard a percentage of the highest and lowest values within each interval. The mean is then computed from the remaining data points, yielding an improved estimate of the true underlying quasi-steady value we seek to characterize with MAMS. The right side image in Figure 20 takes us further down the path past routine trimmed-mean filtering in order to effectively ignore even more of the uninteresting, non-quasi-steady values as well as individually rescaling the vertical limits on per-axis basis. From here, we can compute per-axis medians before versus after the Dragon docking event and when we do, we see the values shown in Figure 21 and in Table 3 below, and notably the main shift in the quasi-steady vector was, as expected from Figure 2 on page 3, discernible shift in the quasi-steady vector along the XZ-plane, including a polarity inversion on the X-axis.

Table 3. Quasi-Steady Vector Components (μg)

Axis	Before	After	Delta
X	0.0612	-0.0651	-0.1263
Y	-0.5170	-0.5133	0.0037
Z	-0.8641	-1.0107	-0.1466

4. CONCLUSION

The Crew-11 Dragon docking to Node 2's zenith port on GMT 2025-08-02 produced a measurable vibratory signature across our distributed network of SAMS sensor heads on the ISS. At lower frequencies (6 Hz passband), the docking impulse was clearly visible in all modules, with sensors located in the Columbus and Kibo modules showing slightly greater response amplitudes. At higher frequencies (nominal 200 Hz passband), localized equipment activity masked the docking signature, most notably from cryocooler operations: ICEBERG-1 in JPM1F6 (ER-4), and GLACIER-2 in LAB1O3 (ER-6), which drove elevated y-limit scaling for sensors es19 and es18, respectively.

These results affirm the importance of multi-sensor, multi-bandwidth monitoring to capture both structural response and operational disturbance context during

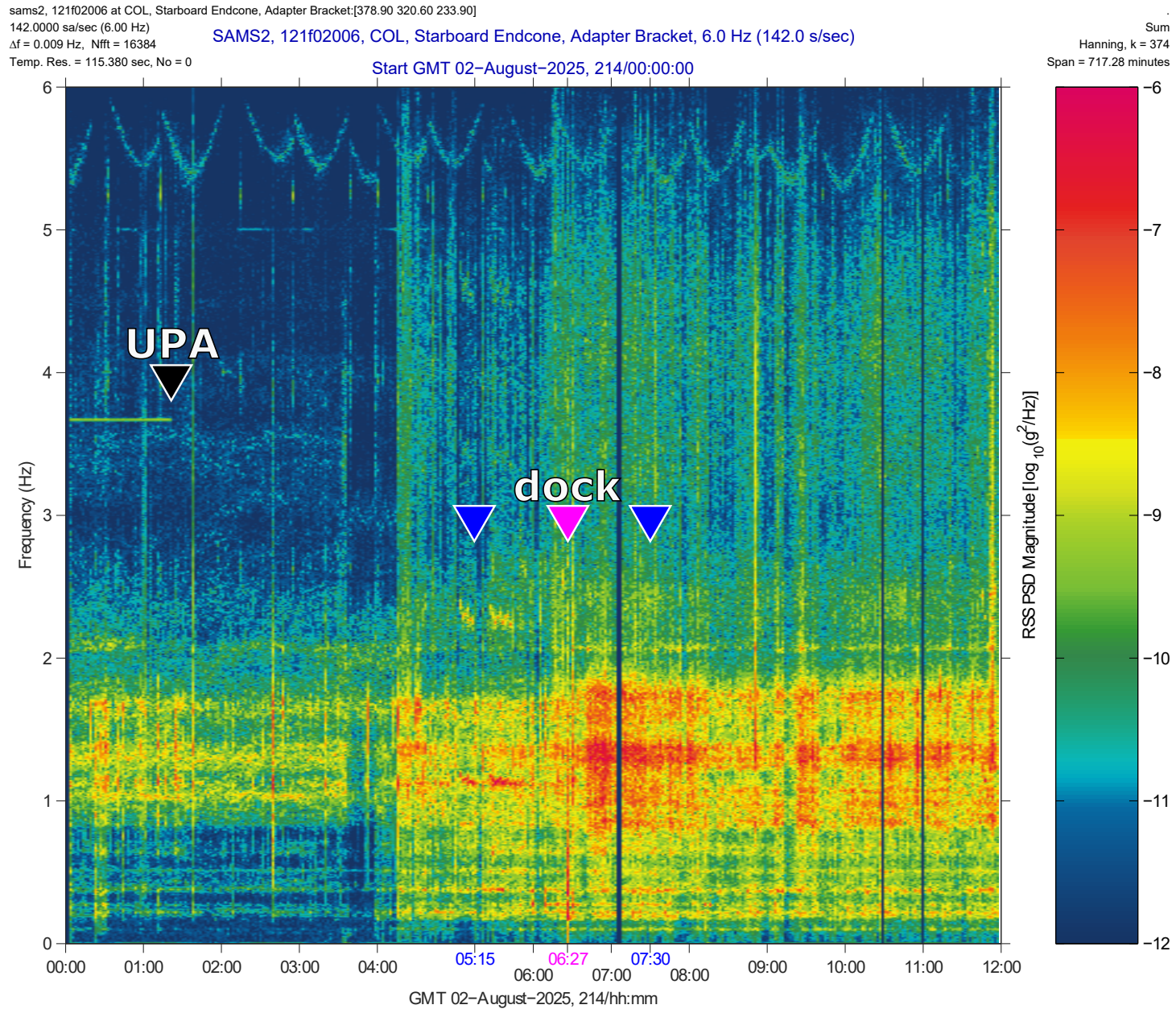
visiting vehicle events such as a Dragon docking. They also highlight the value of correlating vibratory data with operational timelines to distinguish transient docking effects from unrelated equipment activity, albeit in this case, the docking event was shown to stand out when applying a 6 Hz low-pass filter to the as-measured SAMS data.

Analysis of the low-frequency measurements made by MAMS gave further insight as to the impact of the Dragon docking with respect to the quasi-steady regime. A discernible shift in the quasi-steady vector along the XZ-plane, including a polarity inversion on the X-axis.

For further details or clarifications, contact the SAMS team at this email: pimsops@lists.nasa.gov.



Fig. 2: The Logo for Crew-11 Dragon.



VIBRATORY

MODIFIED AUGUST 11, 2025

Fig. 3: 6 Hz, 12-Hour Spectrogram Shows Acceleration Spectrum For Docking Context on GMT 2025-08-02 via Measurements by SAMS Sensor at Columbus Endcone.

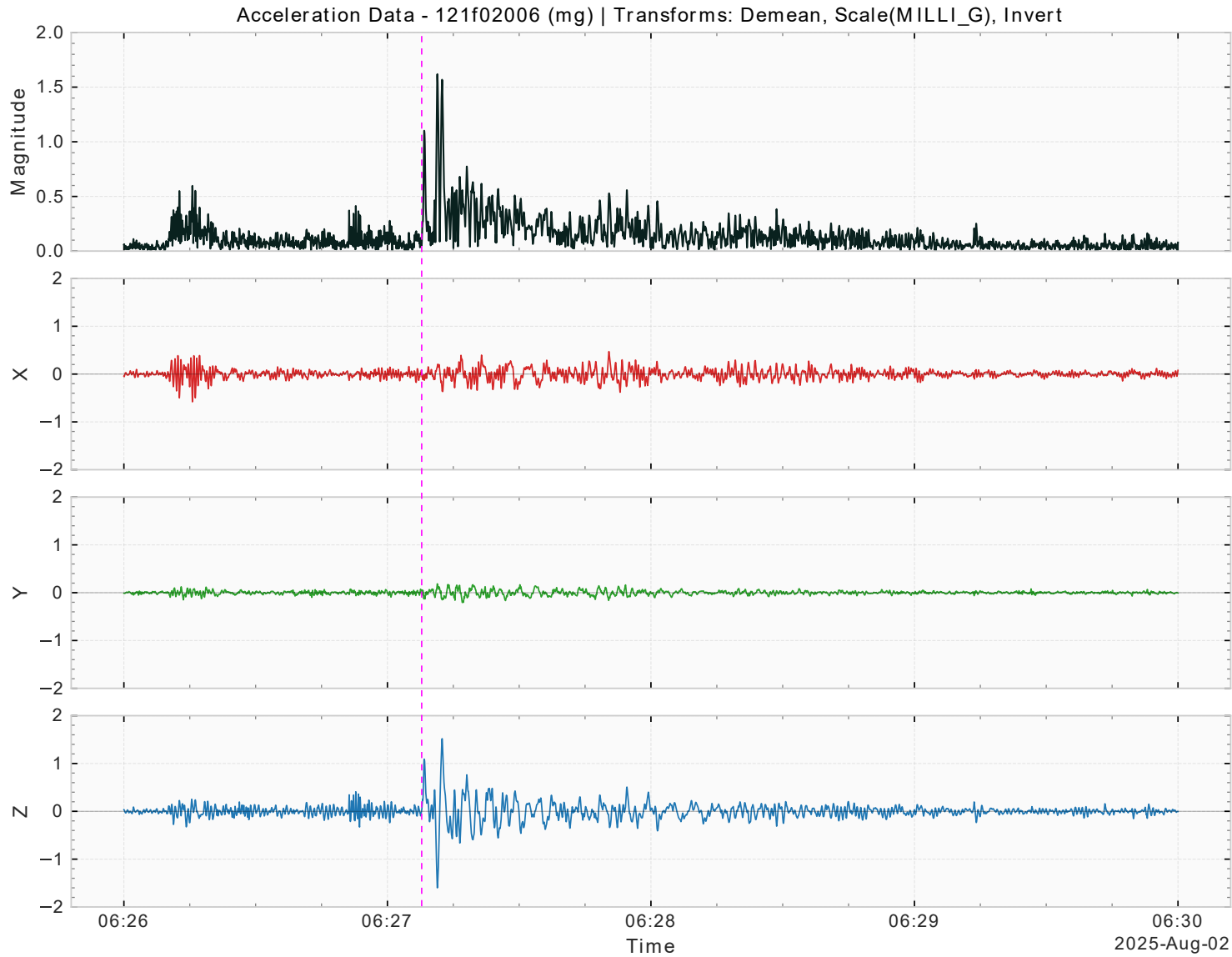


Fig. 4: 6 Hz Low-Pass Filtered Data, 4-Minute Span Around Dragon Docking Event via Measurements by SAMS Sensor at Columbus Endcone.

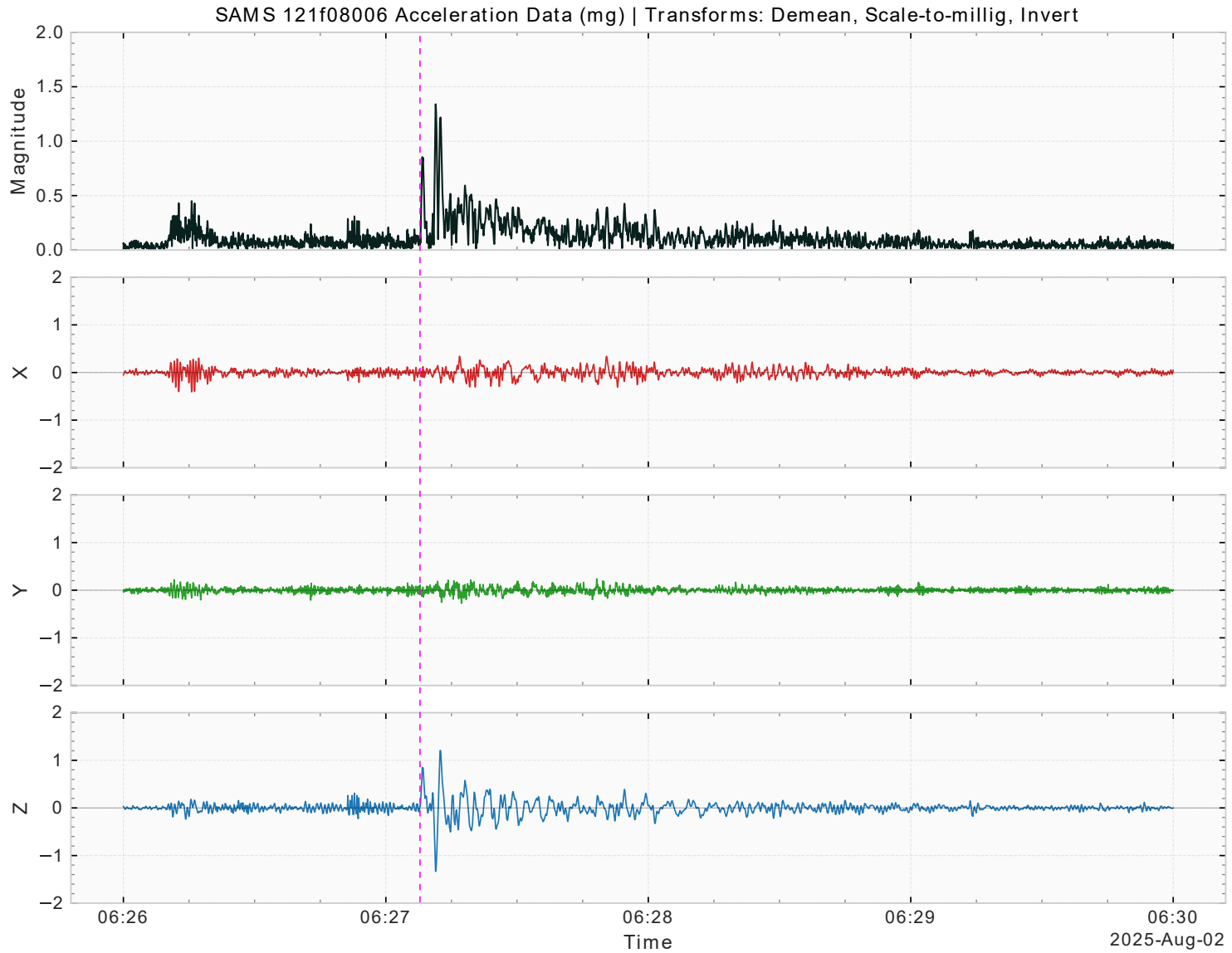


Fig. 5: 6 Hz Low-Pass Filtered Data, 4-Minute Span Around Dragon Docking Event via Measurements by SAMS Sensor at COL1A3.

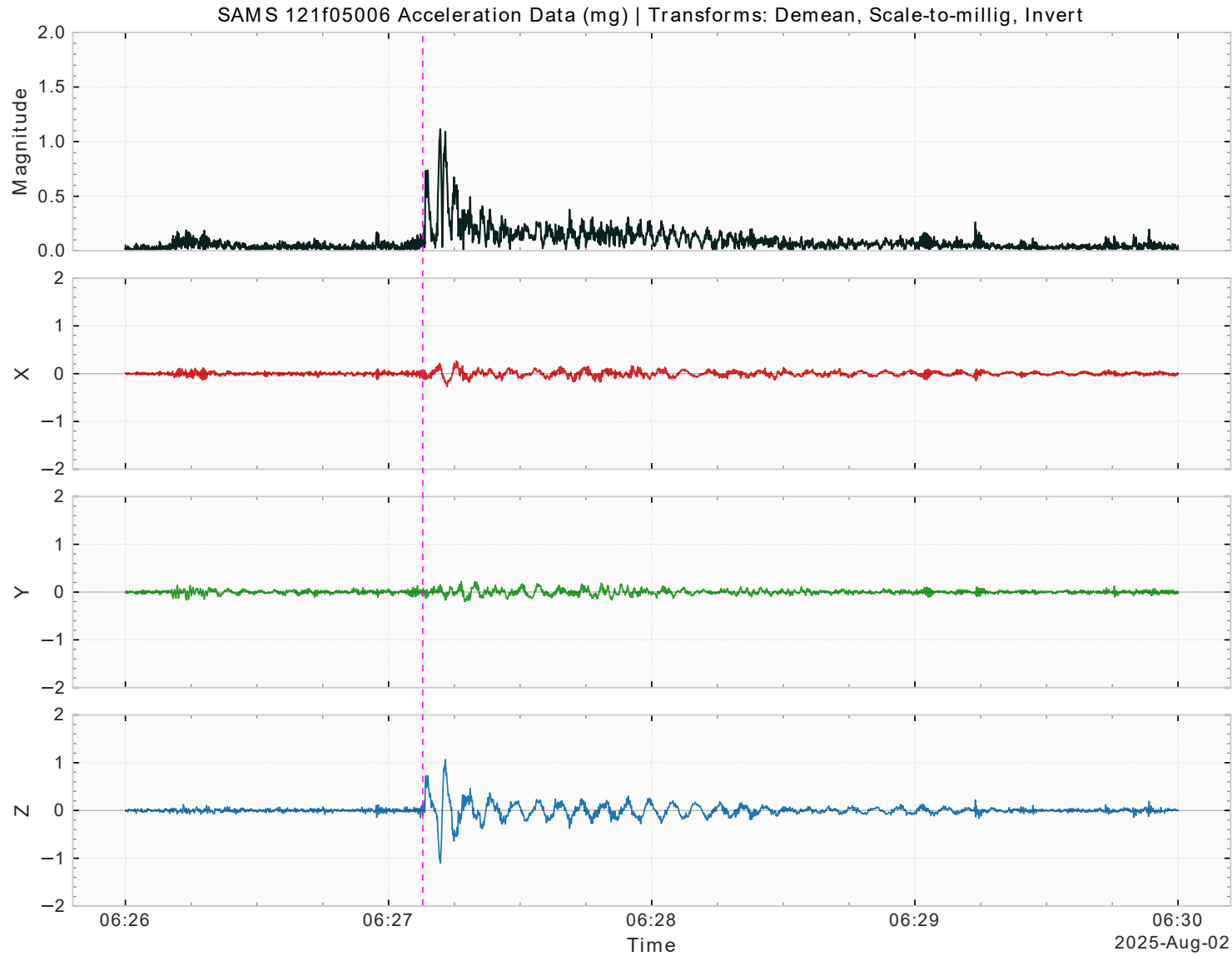


Fig. 6: 6 Hz Low-Pass Filtered Data, 4-Minute Span Around Dragon Docking Event via Measurements by SAMS Sensor at JPM1F1.

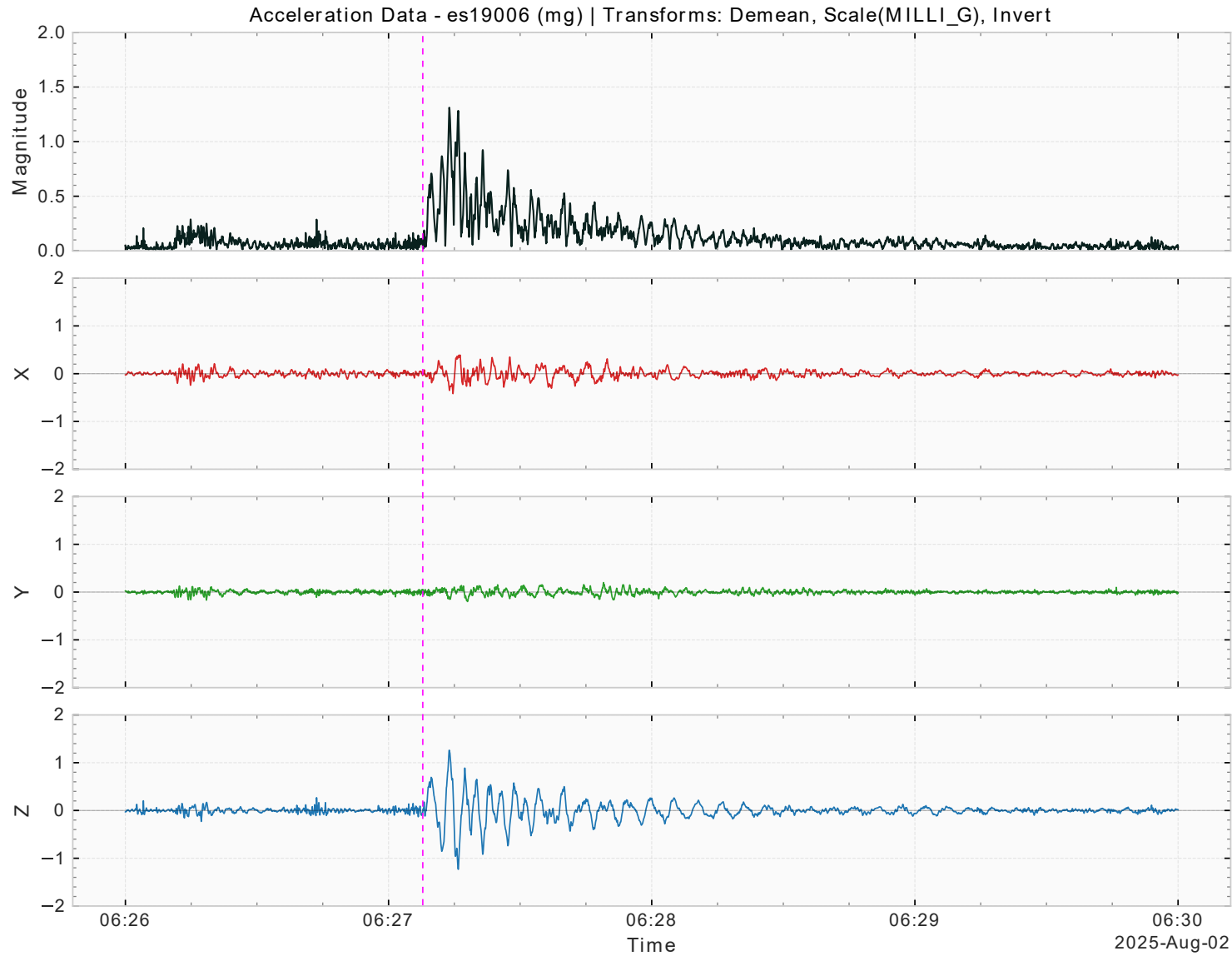


Fig. 7: 6 Hz Low-Pass Filtered Data, 4-Minute Span Around Dragon Docking Event via Measurements by SAMS Sensor at JPM1F6.

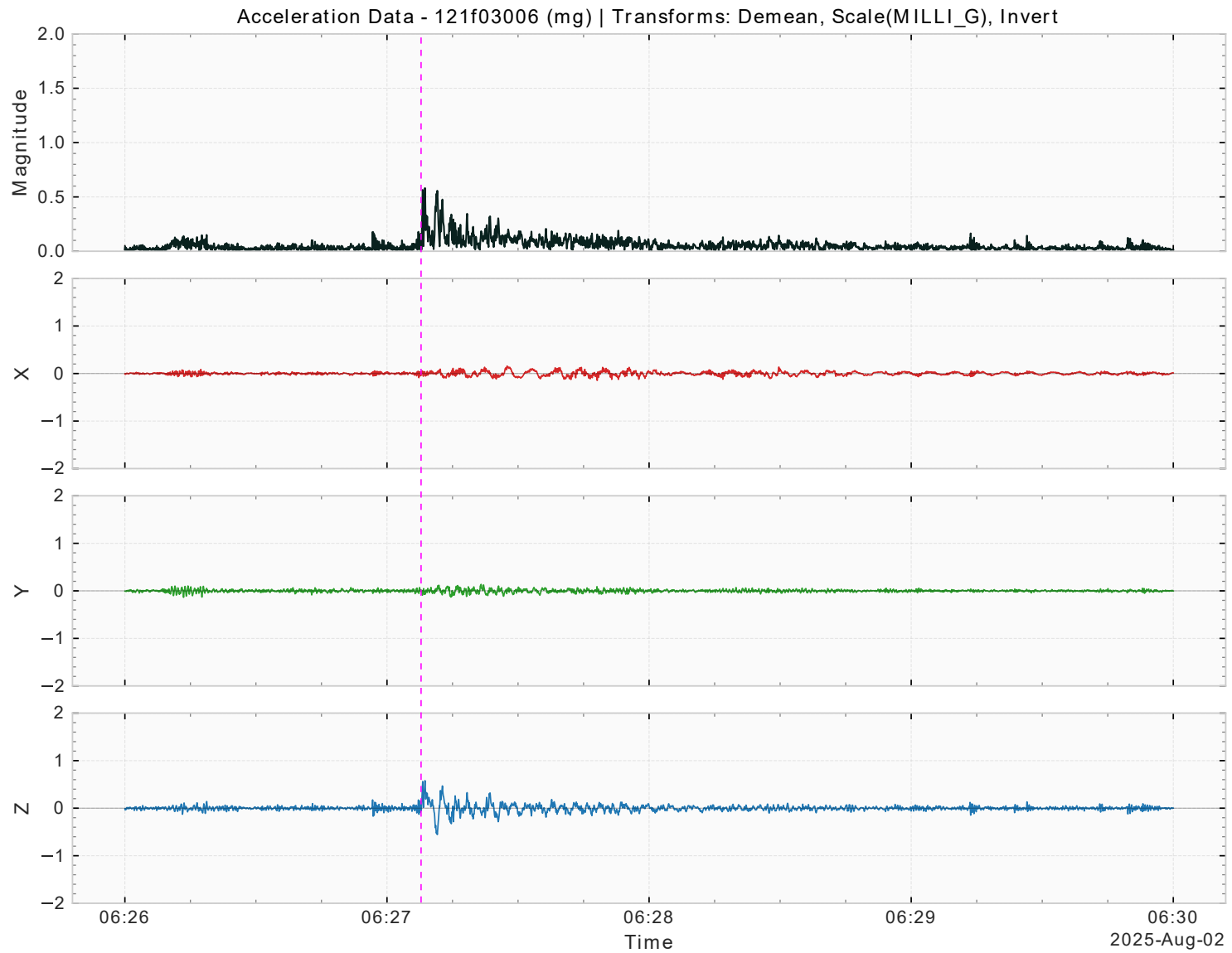


Fig. 8: 6 Hz Low-Pass Filtered Data, 4-Minute Span Around Dragon Docking Event via Measurements by SAMS Sensor at LAB1O1.

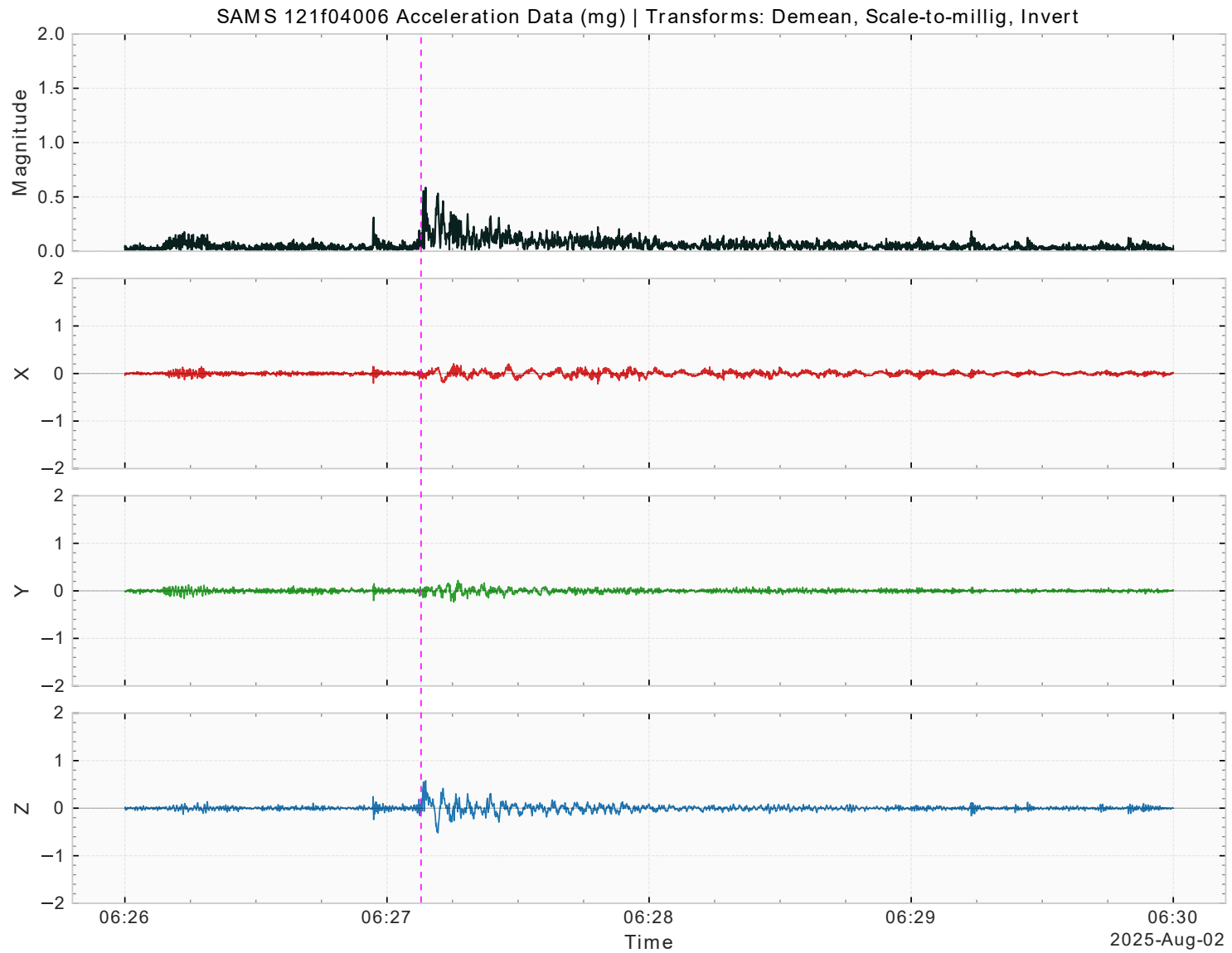


Fig. 9: 6 Hz Low-Pass Filtered Data, 4-Minute Span Around Dragon Docking Event via Measurements by SAMS Sensor at LAB1P2.

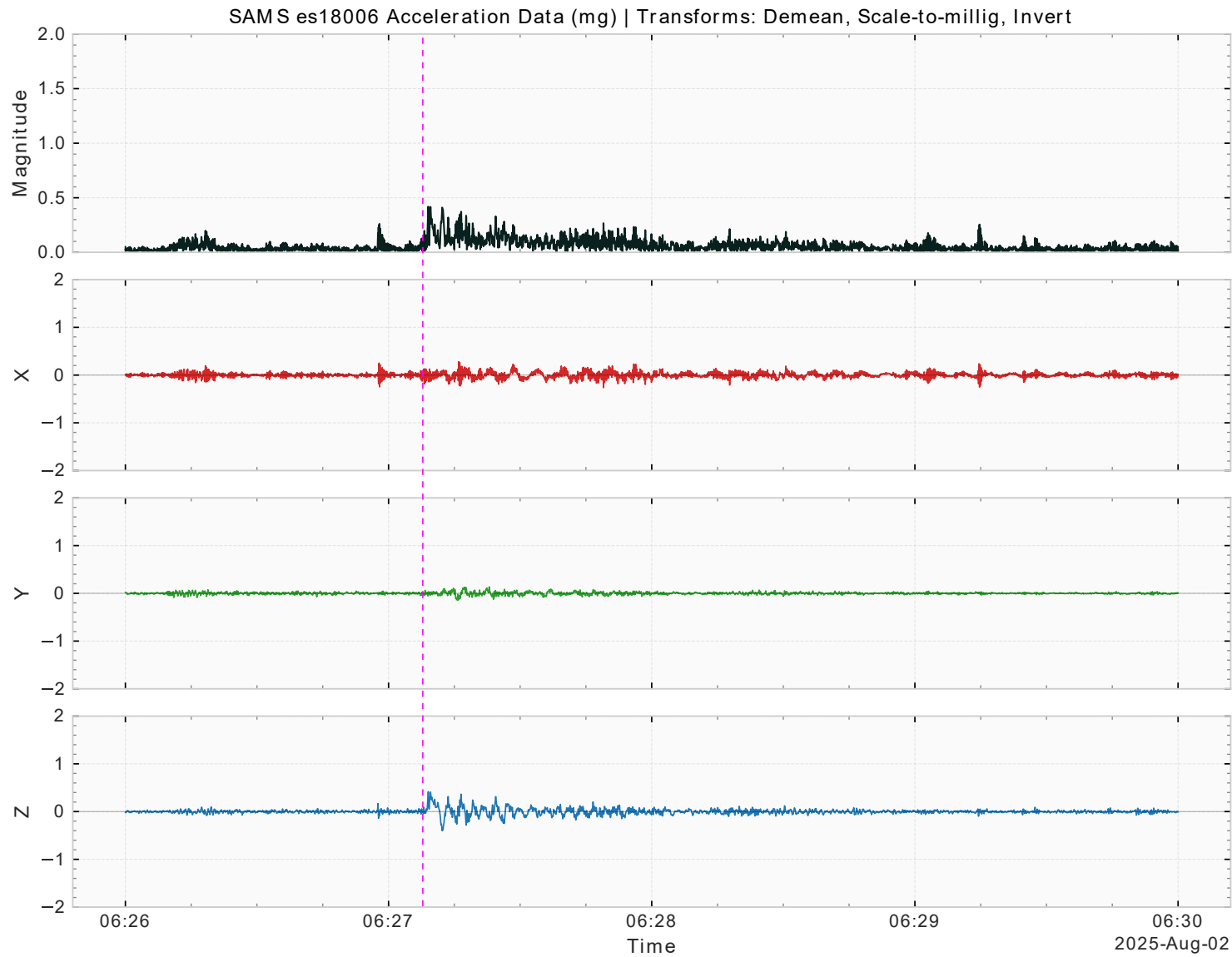


Fig. 10: 6 Hz Low-Pass Filtered Data, 4-Minute Span Around Dragon Docking Event via Measurements by SAMS Sensor at LAB1O3.

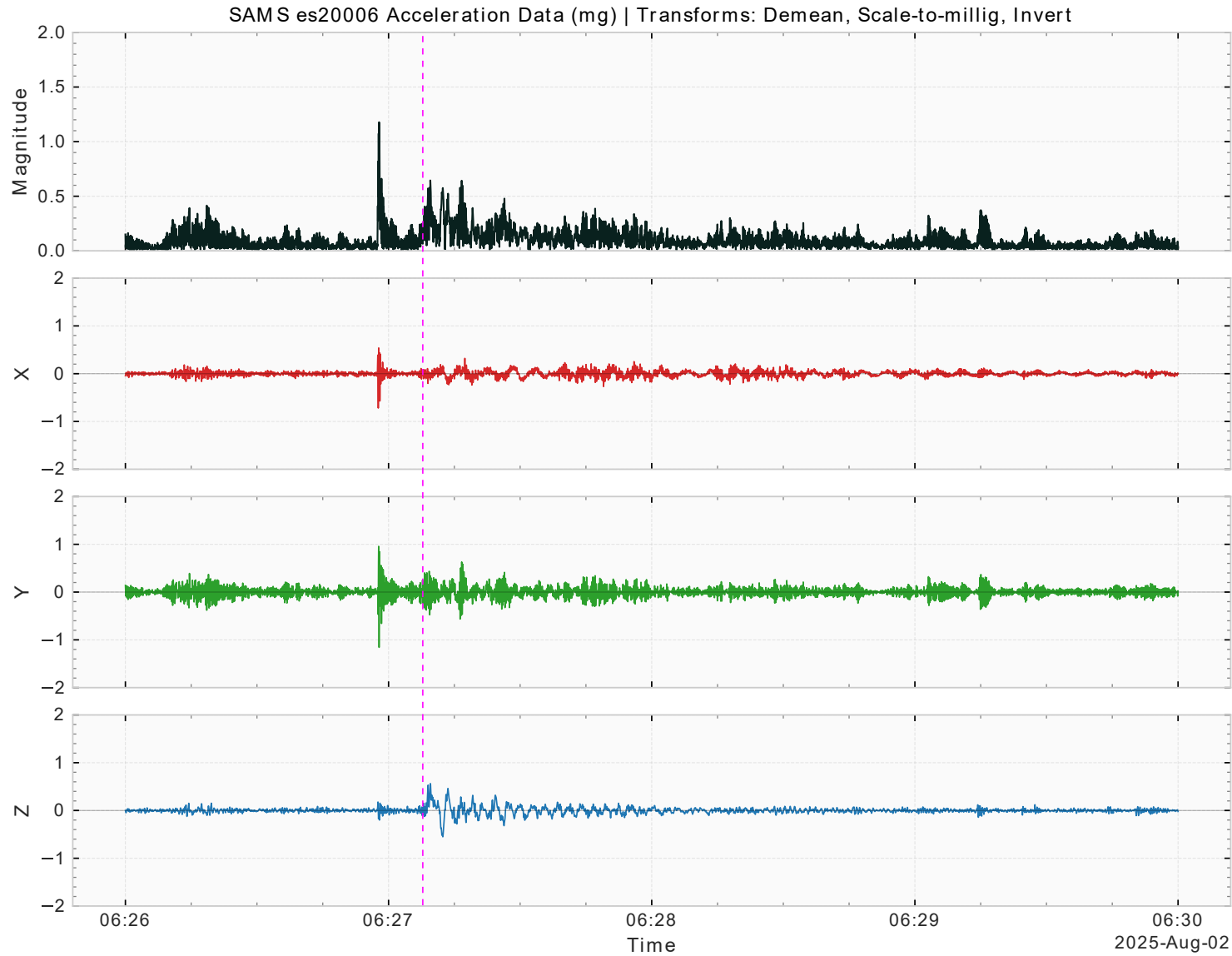


Fig. 11: 6 Hz Low-Pass Filtered Data, 4-Minute Span Around Dragon Docking Event via Measurements by SAMS Sensor at LAB1S2.

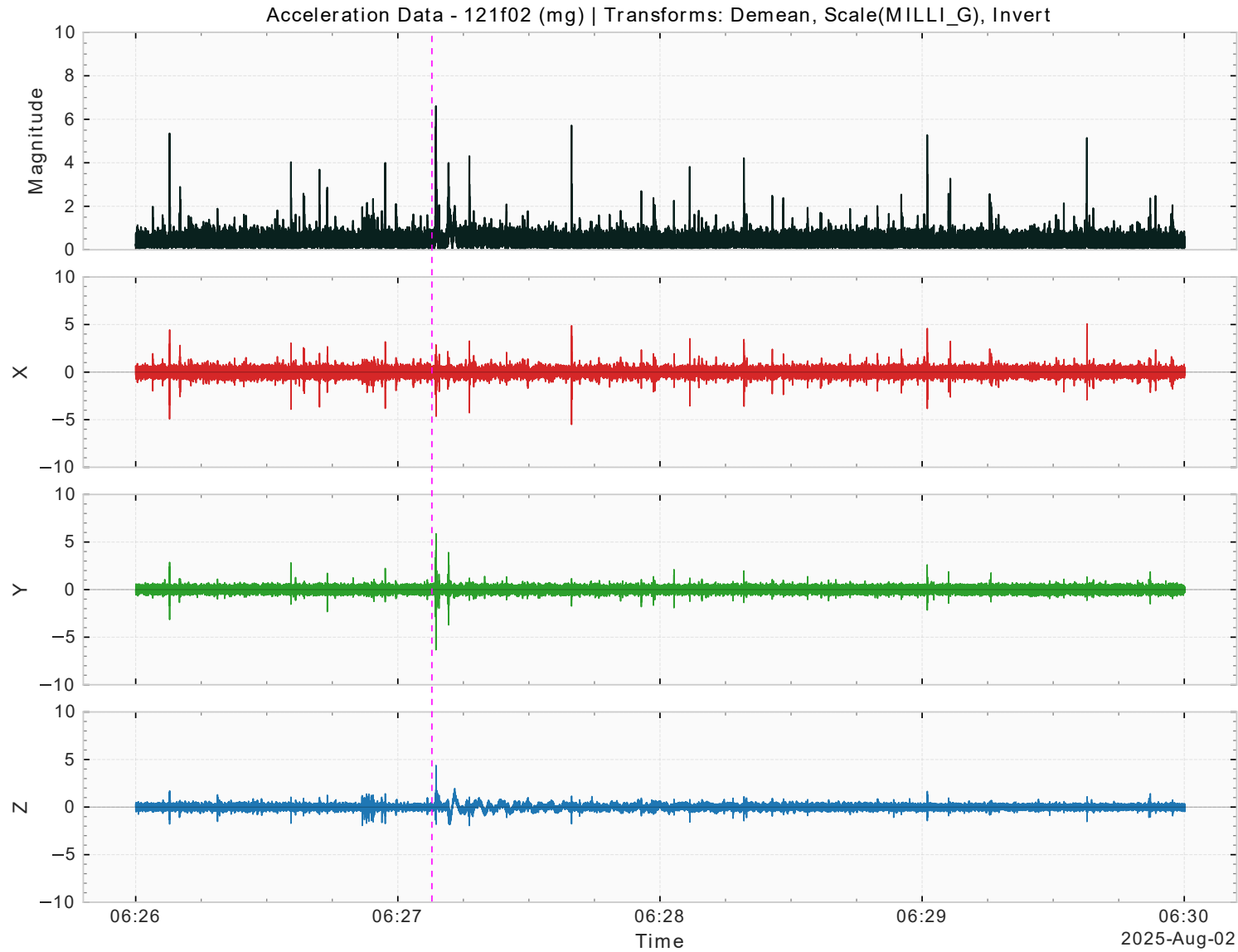


Fig. 12: 6 Hz Low-Pass Filtered Data, 4-Minute Span Around Dragon Docking Event via Measurements by SAMS Sensor at Columbus Endcone.

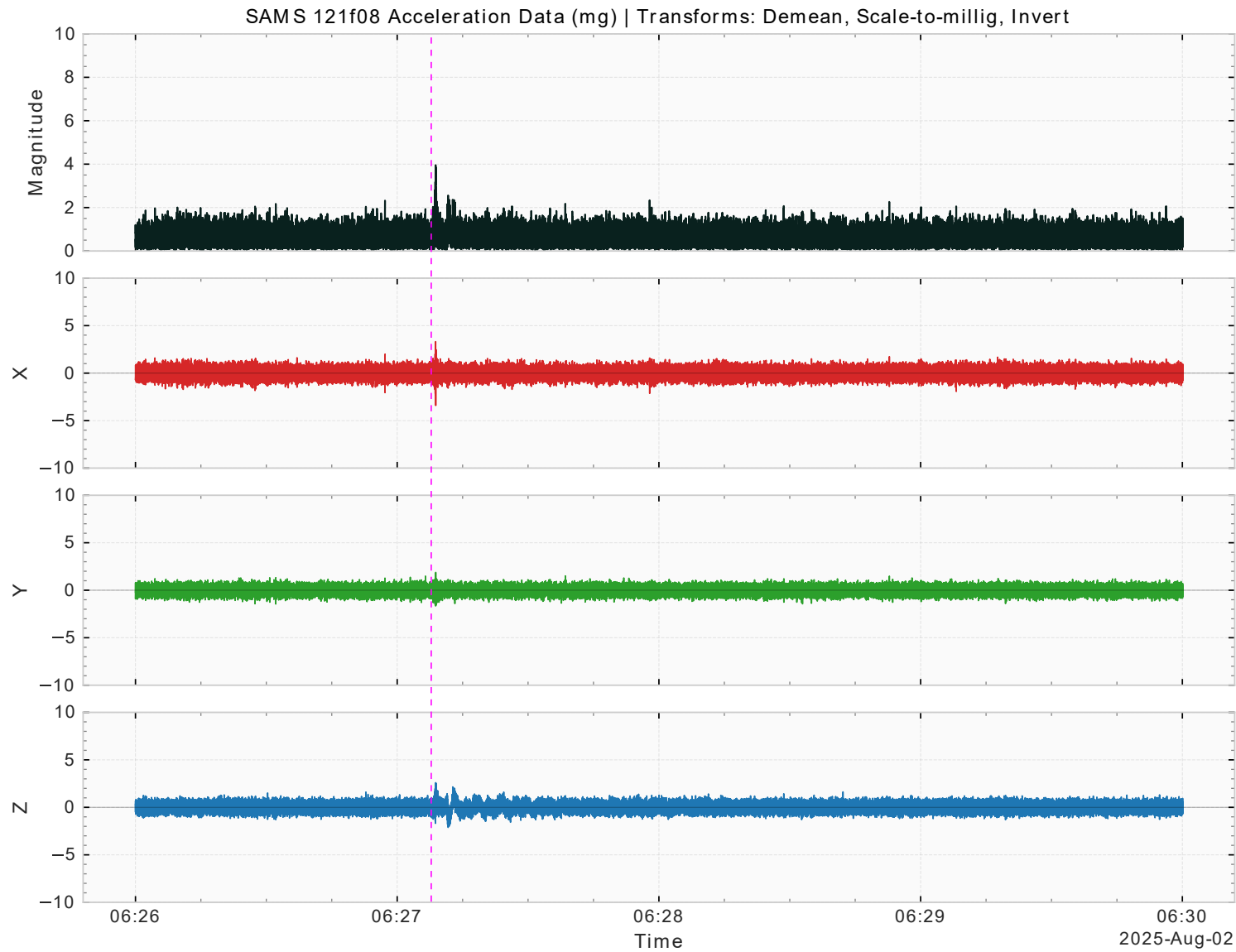


Fig. 13: 6 Hz Low-Pass Filtered Data, 4-Minute Span Around Dragon Docking Event via Measurements by SAMS Sensor at COL1A3.

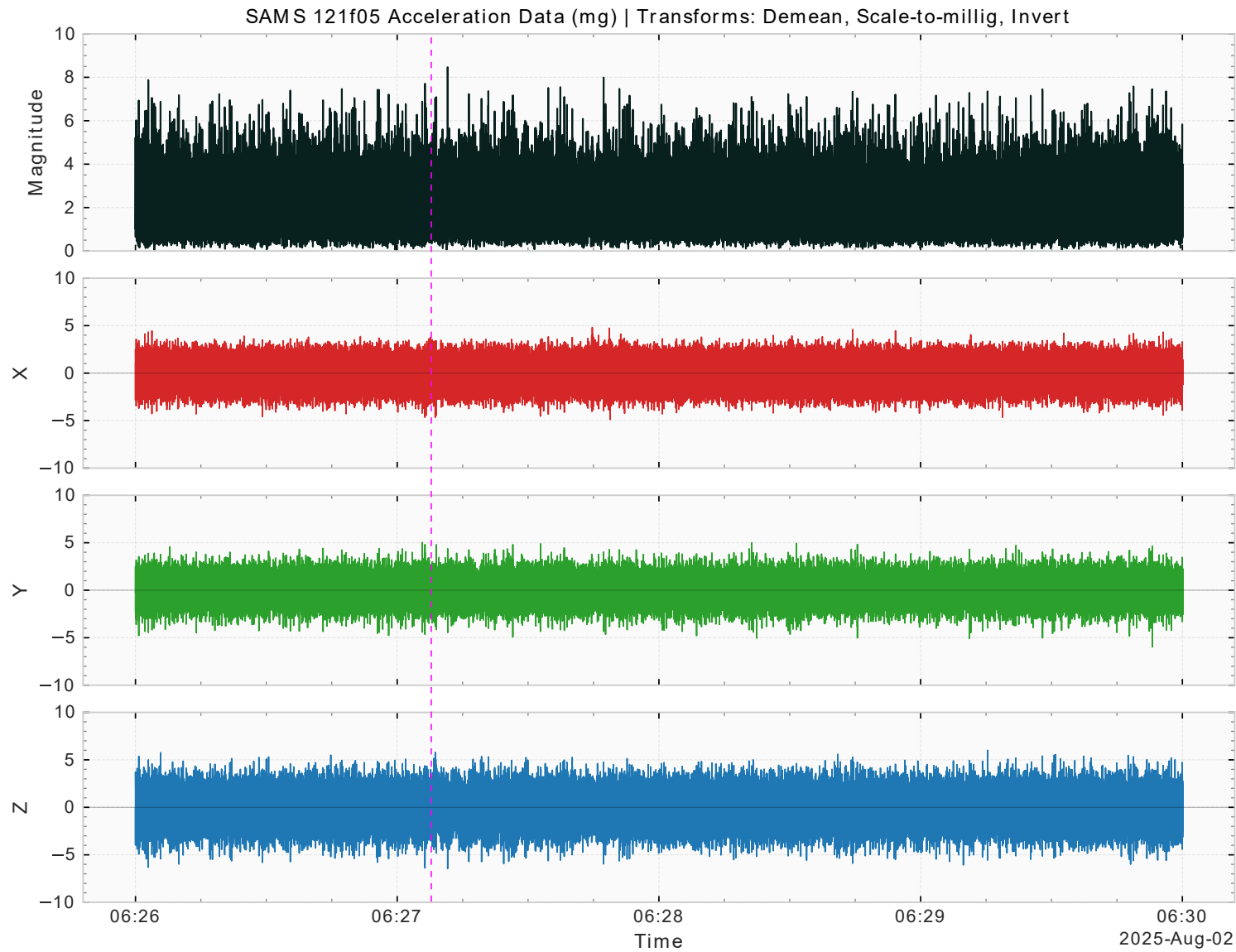


Fig. 14: 6 Hz Low-Pass Filtered Data, 4-Minute Span Around Dragon Docking Event via Measurements by SAMS Sensor at JPM1F1.

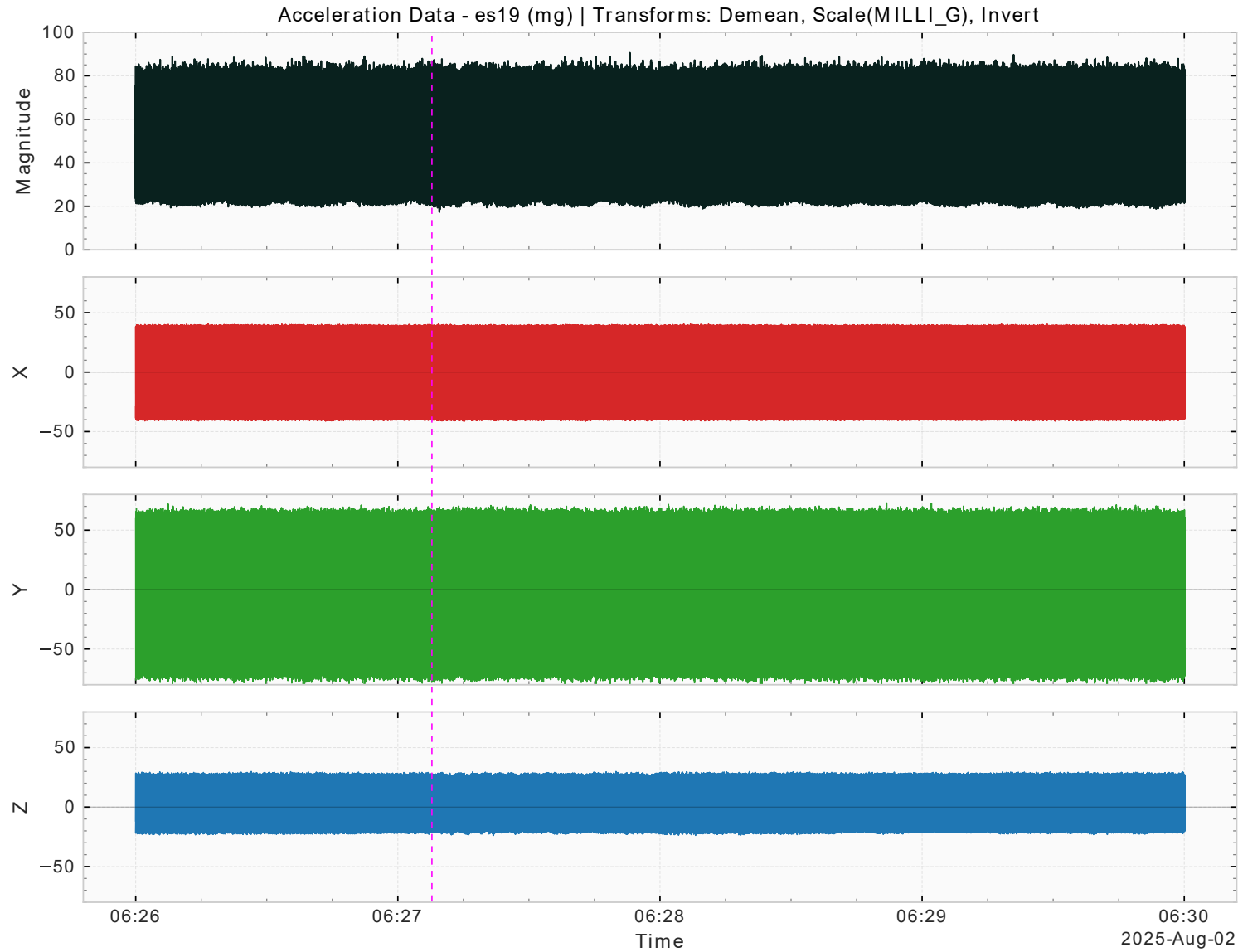


Fig. 15: 6 Hz Low-Pass Filtered Data, 4-Minute Span Around Dragon Docking Event via Measurements by SAMS Sensor at JPM1F6.

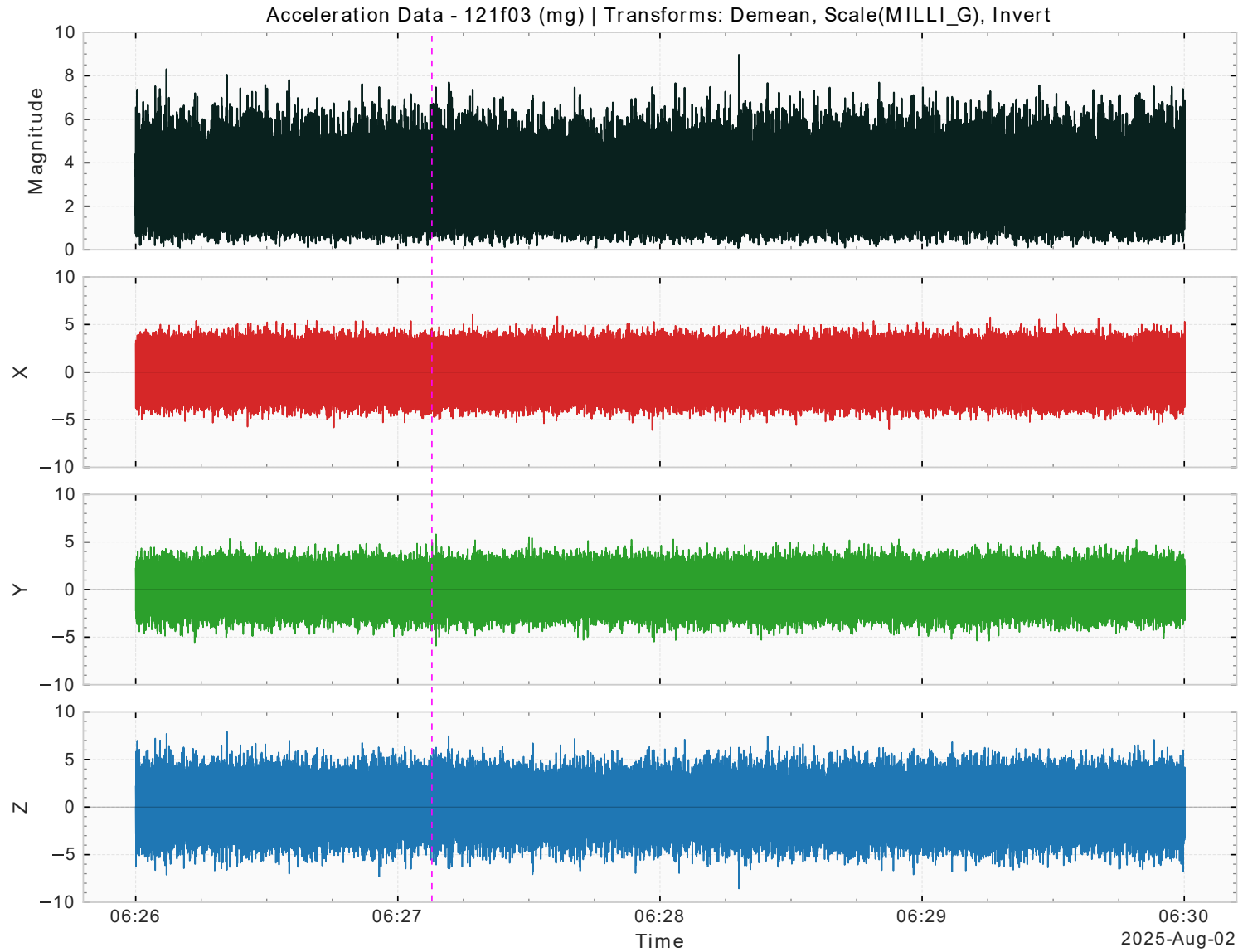


Fig. 16: 6 Hz Low-Pass Filtered Data, 4-Minute Span Around Dragon Docking Event via Measurements by SAMS Sensor at LAB101.

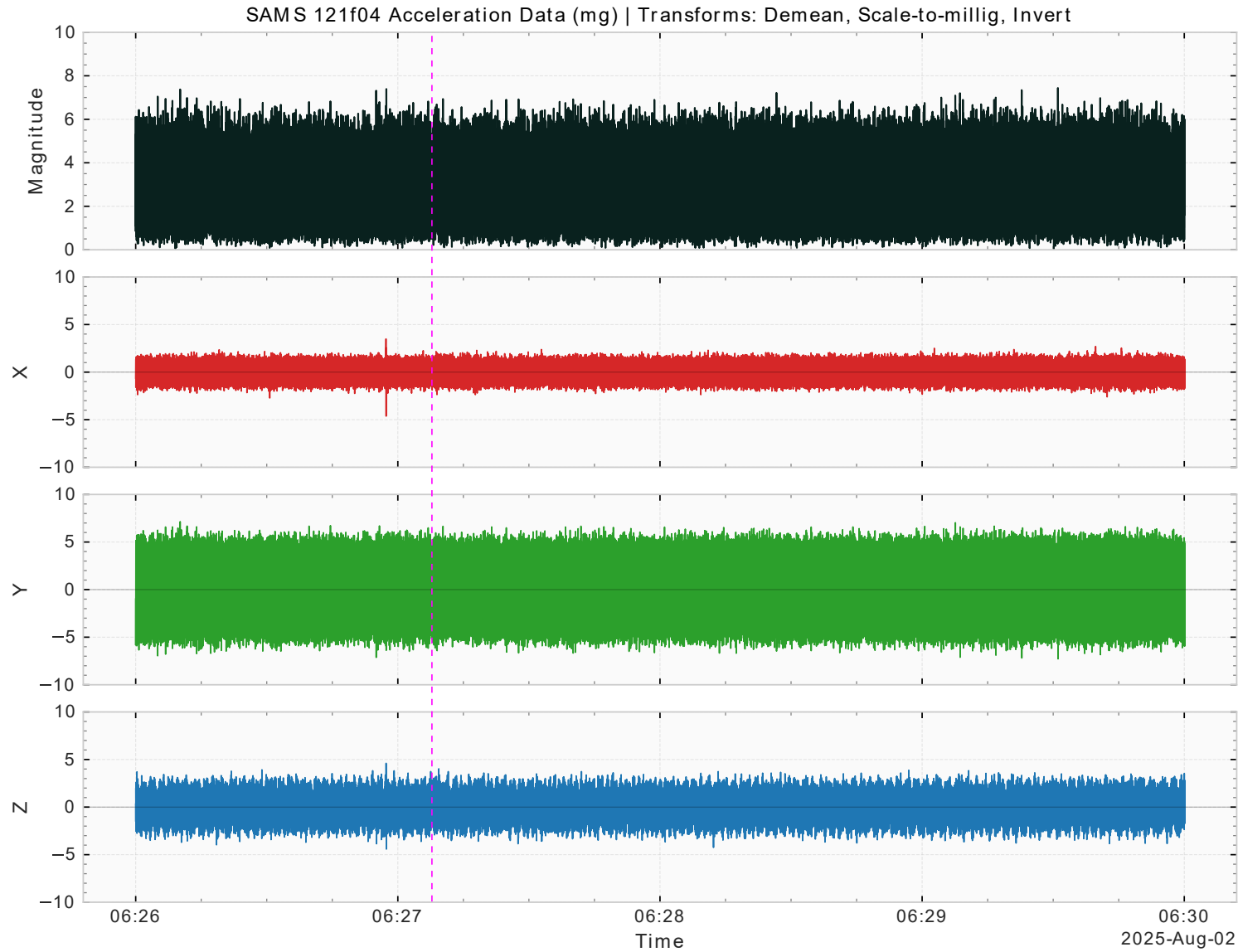


Fig. 17: 6 Hz Low-Pass Filtered Data, 4-Minute Span Around Dragon Docking Event via Measurements by SAMS Sensor at LAB1P2.

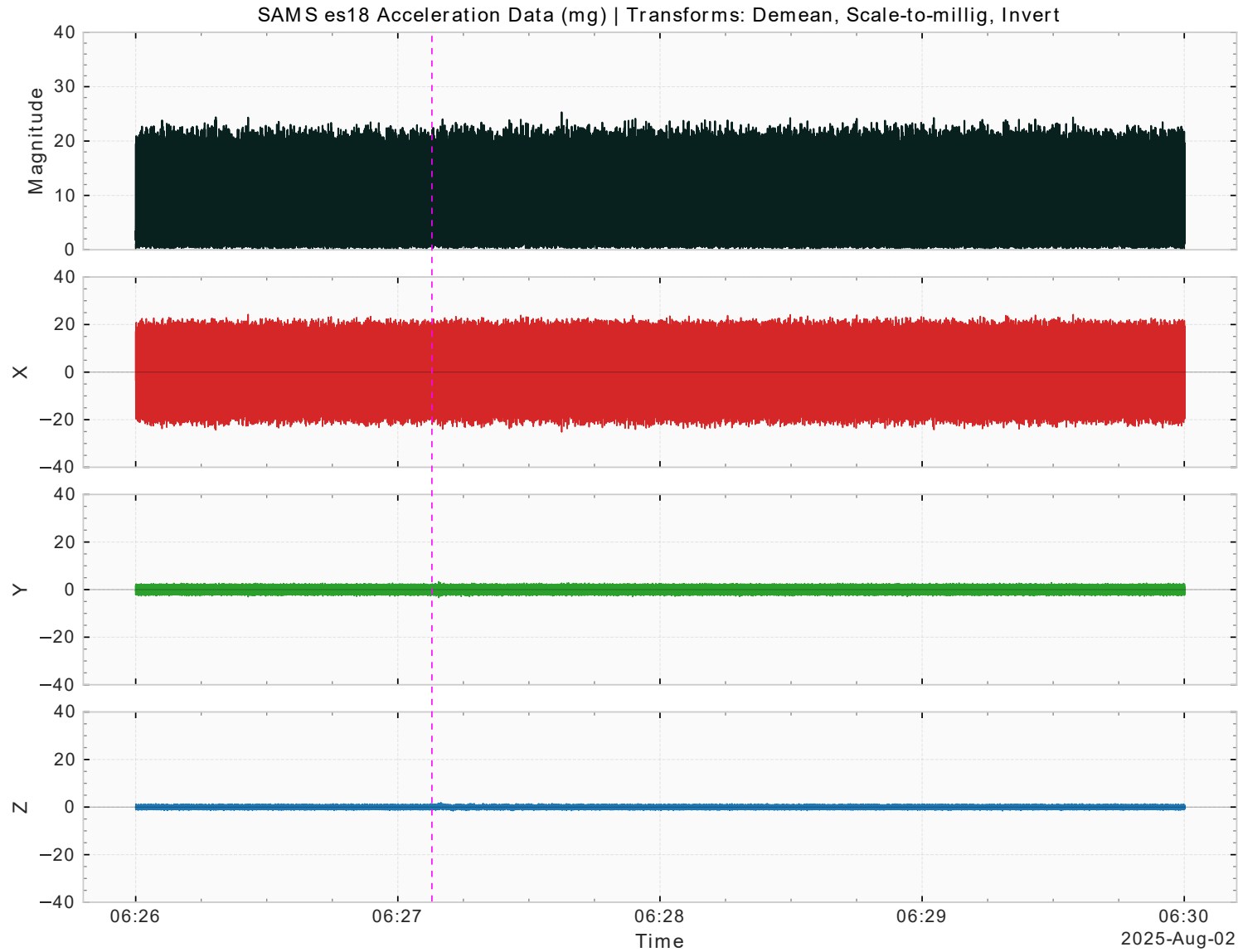


Fig. 18: 6 Hz Low-Pass Filtered Data, 4-Minute Span Around Dragon Docking Event via Measurements by SAMS Sensor at LAB1O3.

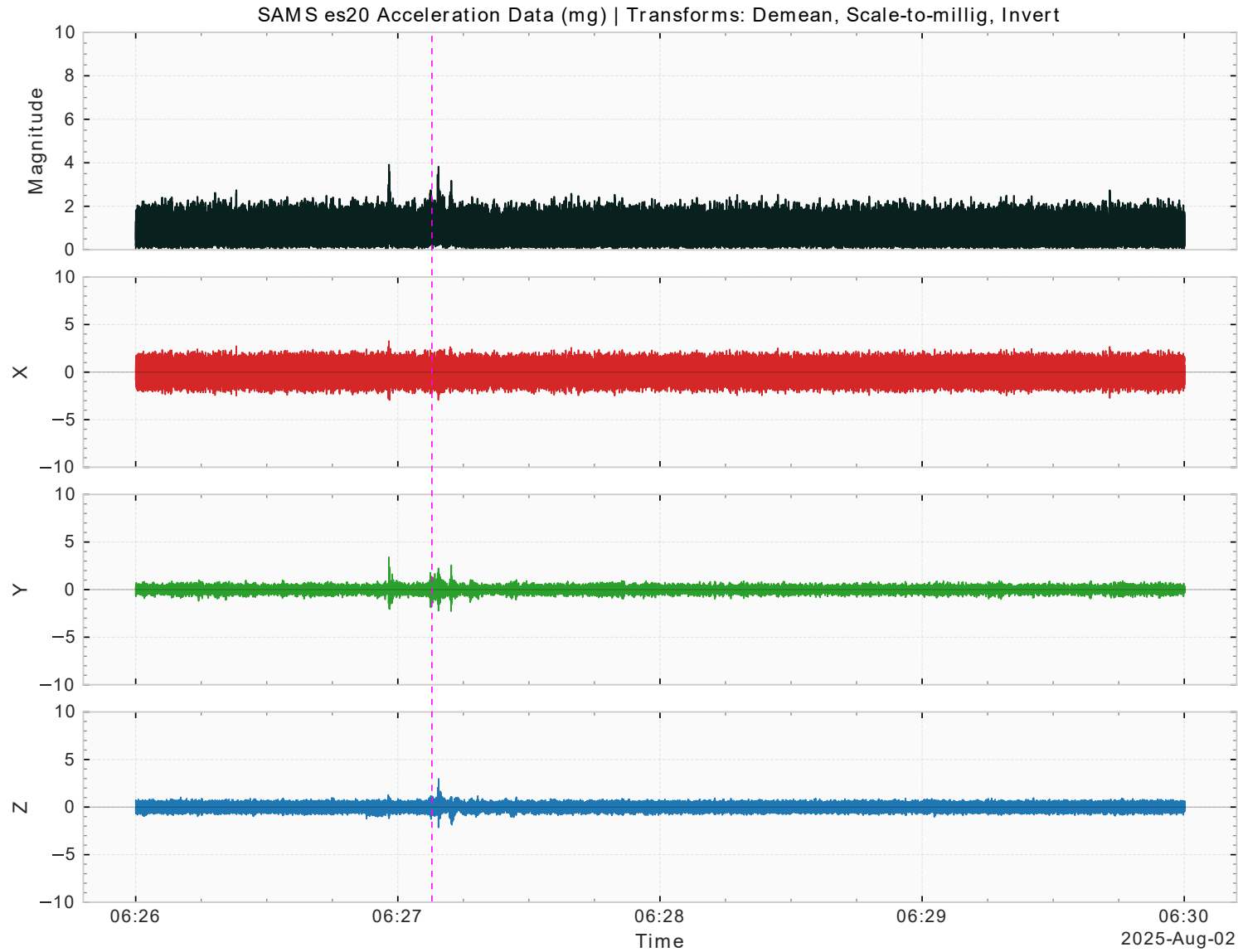


Fig. 19: 6 Hz Low-Pass Filtered Data, 4-Minute Span Around Dragon Docking Event via Measurements by SAMS Sensor at LAB1S2.

mams_ossbtfm at JPM1F1, ER5, Lockers 5,6:[478.83 -117.51 173.87]
0.0625 sa/sec (0.01 Hz)

mams_accel_ossbtfm, JPM1F1, ER5, Lockers 5,6, 0.0 Hz (0.1 s/sec)

SSAnalysis[0.0 0.0 0.0]

mams_ossbtfm at JPM1F1, ER5, Lockers 5,6:[478.83 -117.51 173.87]
0.0208 sa/sec (0.01 Hz)

mams_accel_ossbtfm, JPM1F1, ER5, Lockers 5,6, 0.0 Hz (0.1 s/sec)

SSAnalysis[0.0 0.0 0.0]
Trimmed Mean Filter
Size: 96.00, Step: 48.00 sec.

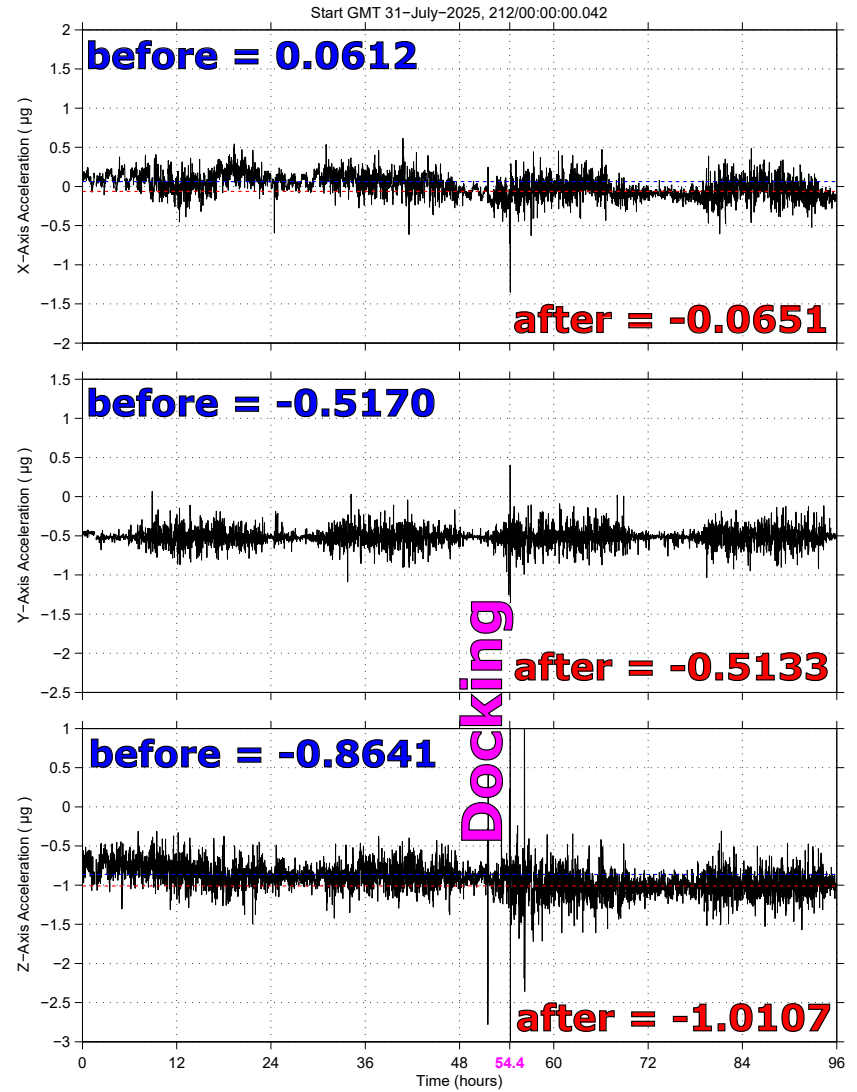
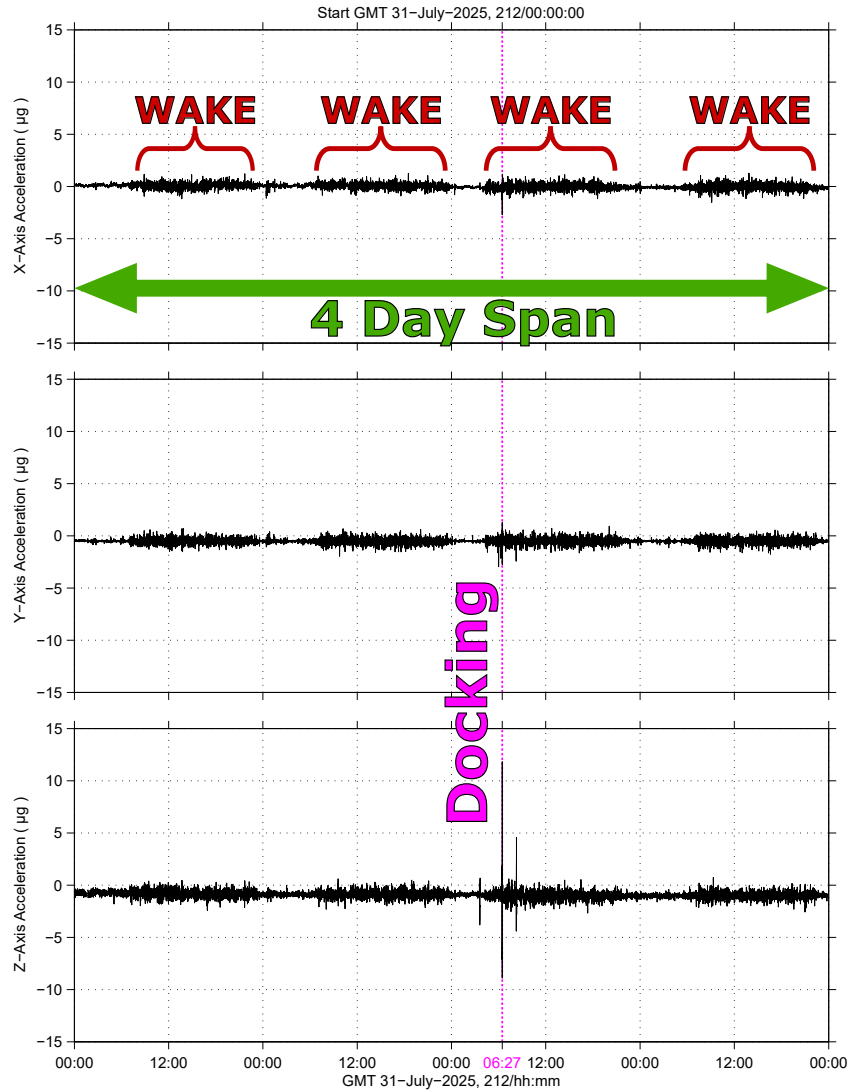


Fig. 20: 4 Days of MAMS Context in JEM: (Left) Per-Axis Best Trimmed-Mean-Filtered, (Right) Per-Axis "More" Trimmed-Mean Filtering & Zoom-in.

mams_ossbmf at JPM1F1, ER5, Lockers 5,6,[478.83 -117.51 173.87]
0.0208 sa/sec (0.01 Hz)

mams_accel_ossbmf, JPM1F1, ER5, Lockers 5,6, 0.0 Hz (0.1 s/sec)

SSAnalysis[0.0 0.0 0.0]
Trimmed Mean Filter
Size: 96.00, Step: 48.00 sec.

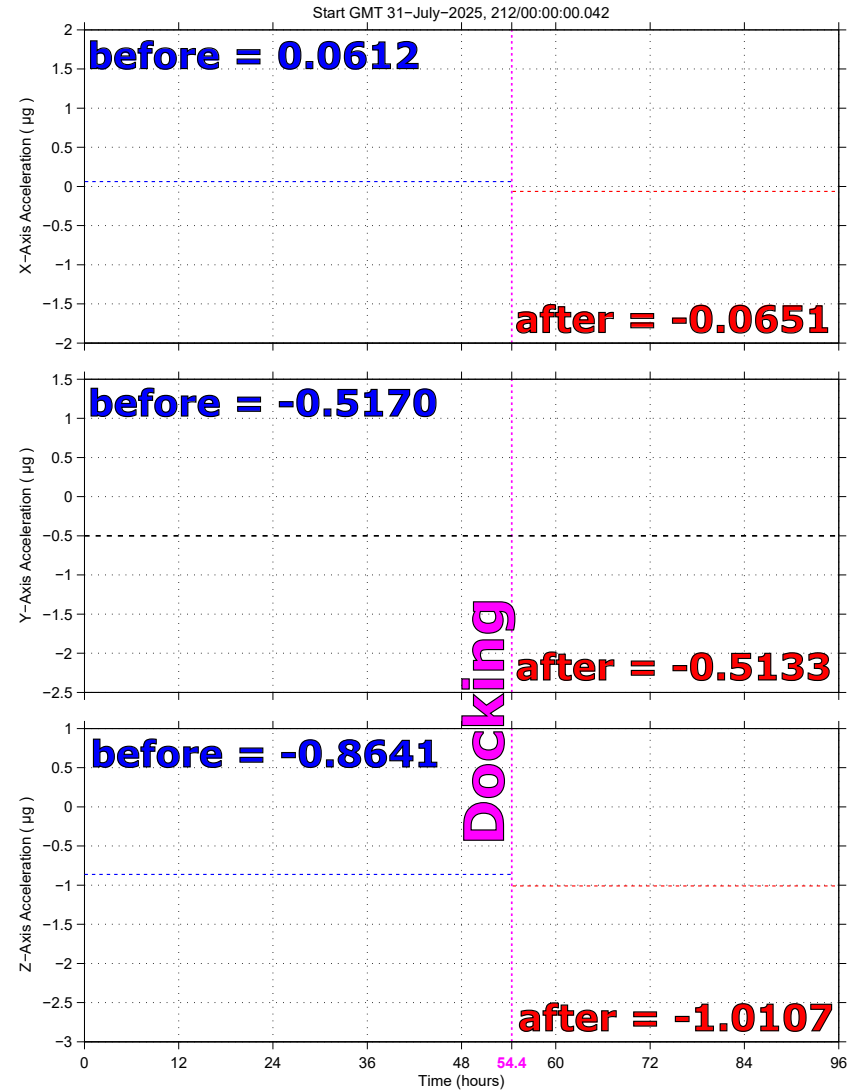


Fig. 21: Same as Right-Side Image on Previous Page, Here Showing Only Median Values Before (blue) vs. After (red) Docking Event.